CHAPTER 7. TECTONO-METAMORPHIC EVOLUTION OF CALC-SILICATE ROCKS

7.1 General

To decipher the temperature and pressure conditions of metamorphism of calc-silicate rocks, conventional thermobarometry was applied. For this purpose Ti-in-biotite thermometer by Henry et al.,(2005) and Silica-Ca-tschermak's-Anorthite (SCAn) geobarometer by McCarthy and Douce (1998) was used. To understand the phase equilibria of these rocks as well as to support the outcomes of thermobarometry, the phase diagrams or the pseudosections were constructed for the representative calc-silcate samples and the chemographic projections were plotted by using Perple_X version 6.8.1 of software (Connolly,2005;Connolly,2009).These studies enabled the understanding of metamorphic facies for these rocks more convincingly.

7.2 Thermobarometry

7.2.1 Ti-in-biotite thermometer

The Ti-in-biotite thermometer of Henry et al.,(2005) has been chosen due to its accuracy and application for calculating peak temperature. It is very recently used single mineral thermometer. In this study the peak temperature of calc-silicate rocks under study has been calculated. This thermometer is based on the relationship between temperature, Ti-content, and Mg/(Mg+Fe) values expressed in the Ti-saturation surface of natural, metapelitic biotite data. It works on the concept that with the increase in temperature, the Ti concentration in magnesian biotites also increases. The expression of this nonlinear trend is as follows:

$T = \{[\ln(Ti) - a - c(X_{Mg})^3]/b\}^{0.333}$, where T is the temperature in ºC, Ti is the apfu normalized to 22 oxygen atoms, X_{Mg} is Mg/(Mg+Fe), and a, b, and c are parameters or surface-fit equation coefficients that represent the fit of the Ti concentration in biotites. Their values are, a = -2.3594, b= 4.6482×10^{-9} and c = -1.7283.The thermometer is empirically calibrated for biotites equilibrated over a temperature range of 480-800ºC and 4-6 kbar pressures, having compositions of Mg/(Mg+Fe) between 0.275 and 1.000 and Ti = 0.04-0.60 apfu. All analysed biotites within these calc-silicates meet the compositional criteria recommended for use of the thermometer. Based on the accumulated uncertainties of the determination of the Ti saturation surface, the precision of the Ti-in-biotite geo-thermometer

is estimated to be ±24 °C at lower temperatures (<600°C), improving to ±12°C at high temperature (>700°C).

Here, the temperature estimates from Ti-in-biotite thermometry were obtained from core and rim analyses on two biotite grains from the sample Ora-03 which is located away from granitic intrusion and two biotite grains in the sample Bor-P10, located near to intrusion (Table7.1). Biotites selected for this study were free of inclusions and devoid of retrogression. Averages of core and rim compositions were employed in calculations. Biotite compositions result in a temperature range of 618-649 ± 24ºC averaging at 618 ± 24ºC in the cores, and 614 ±24 ºC in the rims. The results had a difference of about 31ºC, i.e.649º-618ºC between samples collected from proximity of pluton and those samples collected away from granitic pluton. Thus an average temperature calculated at peak metamorphism for these rocks is around 634 ºC.

Table 7.1: Representative EPMA data of Biotites (core and rim)

Rock no.	Ora-03/2 (Core)	Ora-03/1 (Rim)	Bor-P10/3 (Core)	Bor-P10/2 (Rim)
SiO_2	37.03	34.04	36.25	37.22
TiO_2	1.70	1.68	2.17	2.14
Al_2O_3	16.00	16.59	15.59	15.86
FeO	16.48	15.31	13.46	13.97
MnO	0.18	0.34	0.37	0.31
MgO	14.22	16.52	13.74	14.54
CaO	0.00	0.05	0.00	0.00
Na_2O	0.09	0.09	0.07	0.01
K_2O	9.79	8.39	9.31	9.95
Total	95.49	93.01	96.38	94.00
Ions on the basis of 22(O)				
Si	5.565	5.300	5.55	5.62
Ti	0.197	0.192	0.25	0.243
Al^{IV}	2.434	2.371	2.44	2.379
Al^{VI}	0.399	0.344	0.41	0.442
Fe	2.071	1.993	1.71	1.763
Mn	0.024	0.045	0.035	0.040
Mg	3.185	3.834	3.078	3.274
Ca	0.00	0.009	0.00	0.00
Na	0.027	0.029	0.022	0.003
K	1.877	1.60	1.80	1.917
X_{Mg}	0.60	0.66	0.64	0.65

7.2.2 *Silica–Ca-tschermak's–Anorthite (SCAn) geobarometer*

Some rocks possess no garnet for e.g. rocks from thermal aureoles, massif granulite terrains, tectonically uplifted deep crustal granulites and deep crustal granulite xenoliths but contain pyroxene, plagioclase and quartz (Newton and Perkins,1982).The pressure estimation of such garnet free rocks at peak metamorphism is facilitated with the help of Silica-Ca-tschermak's-anorthite barometer (McCarthy and Douce, 1998).

In order to formulate pressure-sensitive equilibria involving only pyroxene, plagioclase and quartz, the aluminous components in pyroxene (e.g. $CaAl_2SiO_6$, the Ca-tschermak component) must be utililised to balance the aluminium component in plagioclase (Table 7.2).

The pressure-sensitive equilibrium among anorthite, quartz and the Ca-tschermak component in clinopyroxene ($CaAl_2SiO_6$; CaTs), i.e. $CaAl_2SiO_6^{Cpx}+SiO_2^{Qtz} = CaAl_2Si_2O_8^{Pl}$ (SCAn), can be used as a geobarometer in granulites with the proper assemblage, and has been calibrated using mineral composition data from partial melting experiments of natural assemblages and from phase equilibrium experiments on the end-member CMAS system.

Linear least-squares regression analysis of the experimental data resulted in the following empirical expressions for pressure in terms of composition and temperature:

$$P = \frac{5.066\ [\pm 0.760] + \left(\frac{1300\ [\pm 800]}{T}\right) - \ln K}{276\ [\pm 16]} .T\ [\pm 2.5\ \text{kbar}]$$

Or

$$P = \frac{6.330\ [\pm 0.116] - \ln K}{301[\pm 9]} .\ T\ [\pm 1.0\ \text{kbar}]$$

Where, $K = \frac{a_{An}^{Pl}}{a_{CaTs}^{Cpx}}$

The first equation incorporates an enthalpy term, but is less accurate than the second equation, in which the enthalpy of reaction is ignored. Application of these expressions to natural and experimental equilibrium mineral assemblages demonstrates that the empirical barometers are applicable over a wide range of pressures (≥4 kbar), temperatures (≥700 °C) and bulk compositions (Mg# ≥32.5) (McCarthy and Douce, 1998).

The reaction (above) in which quartz and Ca-tschermak component of clinopyroxene combine to form anorthite fixes the chemical potential of Ca-tschermak component and has been studied experimentally by Hays (1966), Hariya and Kennedy (1968), Wood (1976, 1978, 1979) and Gasparik (1984a,b, 1986).

Inadequacies of nonideal ca-tschermak solution models result errors in the determination of pressure(Raith et al., 1983) but in the absence of reliable solution models for aluminous pyroxenes, empirical methods have been used to calibrate the clinopyroxene–plagioclase–quartz barometer (above reaction).

This study involves the determination of the pressure conditions of calc-silicate samples under investigation. On the basis of representative clinopyroxene (Ca-tschermak component) and plagioclase analyses, the calculations for mole fractions and ideal activity expression have been carried out by using the following formulae:

Mole fractions and ideal activity expression for CaTs and An.

Clinopyroxene activity–composition relationships (Wood, 1979**)**

Cation assignment (recalculated on the basis of six oxygens)

$Al^{iv} = 2- Si$, $X\ Al^{M1} = Al–Al^{iv}$, $X\ Ca^{M2} = Ca$, $X\ Si^{iv} = Si/2$, $X\ Al^{iv} = (2–Si)/2$

$\mathbf{a_{CaTs}^{Cpx}} = 4\ XCa^{M2}\ XAl^{M1}\ XAl^{iv}\ XSi^{iv}$

Plagioclase activity–composition relationships (Holland and Powell, 1992)

X_{An}= Ca/ (Ca+Na+K), $X_b = 0.12+0.00038\ T$, $X_{An,c} = X_{An}\ (1+X_{An})^2 \cdot 1/4$, $I_{An} = -RT \ln (X_{An,c}/X_{An})-(W_c-W_i)\ (1-X_b)^2$, $W_c = 1070.0$ J mol−1, $W_i = 9790.0$ J mol−1

$\mathbf{a_{An,c}^{Pl}} = X_{An,c} \exp (1/RT\ [W_c\ (1-X_{An})^2+I_{An}])$

$$K = \frac{a_{An}^{Pl}}{a_{CaTs}^{Cpx}}$$

Therefore, using 2nd eq. (as it is more accurate than eq.1) for pressure,

$$P = \frac{6.330[\pm 0.116] - \ln K \,.\, T\ [\pm 1.0\text{kbar}]}{301[\pm 9]}$$, where temperature is in K.

Putting the respective values in above equation the pressure value acquired is 1.1 kbar.

Table 7.2 : Representative EPMA data of Clino-pyroxene and Plagioclase feldspar

Clino-pyroxene		Plagioclase feldspar	
Rock no.	Ora-03/2	Rock no.	Prs-10/2
SiO_2	48.5401	SiO_2	46.93
TiO_2	1.3001	Al_2O_3	29.18
Al_2O_3	1.8878	FeO	1.13
Cr_2O_3	3.6906	CaO	20.96
FeO	6.6518	Na_2O	1.18
MnO	0.3998	K_2O	0.24
MgO	11.2834	BaO	0.17
CaO	23.4351	SrO	0.00
Na_2O	0.379		
K_2O	0.0841		
Total	97.65	Total	99.82
Ions on the basis of 6(O)		Ions on the basis of 32 (O)	
Si	1.87	Si	8.96
Ti	0.037	Al	7.32
Al	0.086	Fe(ii)	0.20
Cr	0.112	Ca	4.78
Fe(ii)	0.21	Na	0.48
Mn	0.013	K	0.065
Mg	0.65	Ba	0.014
Ca	0.97	Sr	0.00
Na	0.028		
K	0.0041		
X_{Mg}	0.75		
Pyx. components		Feldspar components	
Wo	49.68	An	89.63
En	38.95	Ab	9.13
Fs	10.57	Or	1.22

7.3 Phase diagrams/ pseudosections

Phase diagrams were computed as a function of calc-silicate bulk rock compositions via a free energy minimization strategy implemented in Perple_X version 6.8.1 (Connolly, 2005; Connolly, 2009). Thermodynamic data from the Holland and Powell dataset (1998), updated in 2003, was employed for end-member calculations. Mixing properties of

phases involving solid-solution were included in calculations, employing the solution model of Holland and Powell (1996) for clinopyroxene, Wei and Powell (2003) and White et al., (2003) for calcic-amphibole, Newton et al., (1980) for plagioclase, and Waldbaum and Thompson (1968) for potassium-feldspar. Pseudosections were modelled in the system:K_2O-Na_2O-CaO-MgO-FeO-TiO_2-Al_2O_3-SiO_2-H_2O-CO_2(KNCFMASTCH). Saturation of quartz (SiO_2) was assumed in calculations for quartz-bearing samples with bulk SiO_2 greater than 50 weight percent.

Isobaric T-X(CO_2) pseudosections were calculated at 1kbar of pressure assuming stability of a binary H_2O-CO_2 fluid, where X(CO_2) represents the mole fraction of species CO_2 relative to H_2O + CO_2 in the fluid. T-X(CO_2) diagrams portray mineral equilibria as a function of temperature and fluid composition. Fields of stability between different equilibrium assemblages can be shown by these diagrams for a single bulk rock composition. Phase equilibrium calculations involving binary H_2O-CO_2 fluids were performed using the CORK equation of state from Holland and Powell (1991).

Pseudosections for samples, viz. Ora-03, Jtng-09 and Tlwd-14 were calculated for a temperature range of 320-600ºC while for a sample Bor-P10, it was calculated for a temperature range of 320-650°C as this location is very near to granitic intrusion. Fluid compositions range assumed between 0 and 1 for X(CO_2) and pressure as 1 kbar.

As according to (Bucher and Grapes, 2011) constant pressure of 1 kbar is considered for shallow level contact aureole and as mentioned earlier, these rocks offer the evidences of contact metamorphism.

The equilibrium assemblage amph +cpx + mc +qz +cal + ttn + bt was observed in thin section of Ora-03 sample and used in pseudosection calculations. In the pseudosection (Fig.7.1), calcic amphibole and cpx are in equilibrium within the assemblage observed as 'amph pl pl cpx fa osm1 sa ilm' which derived the stability field with temperature range of 500°-560°C and fluid compositions of X(CO_2) >0.90. Calcic amphibole (actinolite) appears at almost 380°C and destabilizes above 470°C with the appearance of cpx (diopside) which defines the minimum temperature required for its formation and at X(CO_2) range = 0.9 to 1. Calcic amphibole occurs at most of the specified conditions. K-feldspar (microcline) is predicted in nearly all stability fields upto 500°C.Above 500°C microcline becomes unstable and instead of it sanidine appears.Quartz is stable in the whole T-X(CO_2) range of interest. Carbonate-bearing fields become ubiquitous at wide range of temperatures, i.e. ~320°-404°C and almost at all fluid compositions with calcite, ankerite, dolomite and siderite representing a part of protolith composition. Titanite is stable at temperature 320°-425° C and at lower

$X(CO_2)$ conditions, i.e.< 0.3. Phlogopite appears at ~360°C and is stable as part of K-feldspar bearing assemblages even at higher temperatures and almost at all fluid compositions.

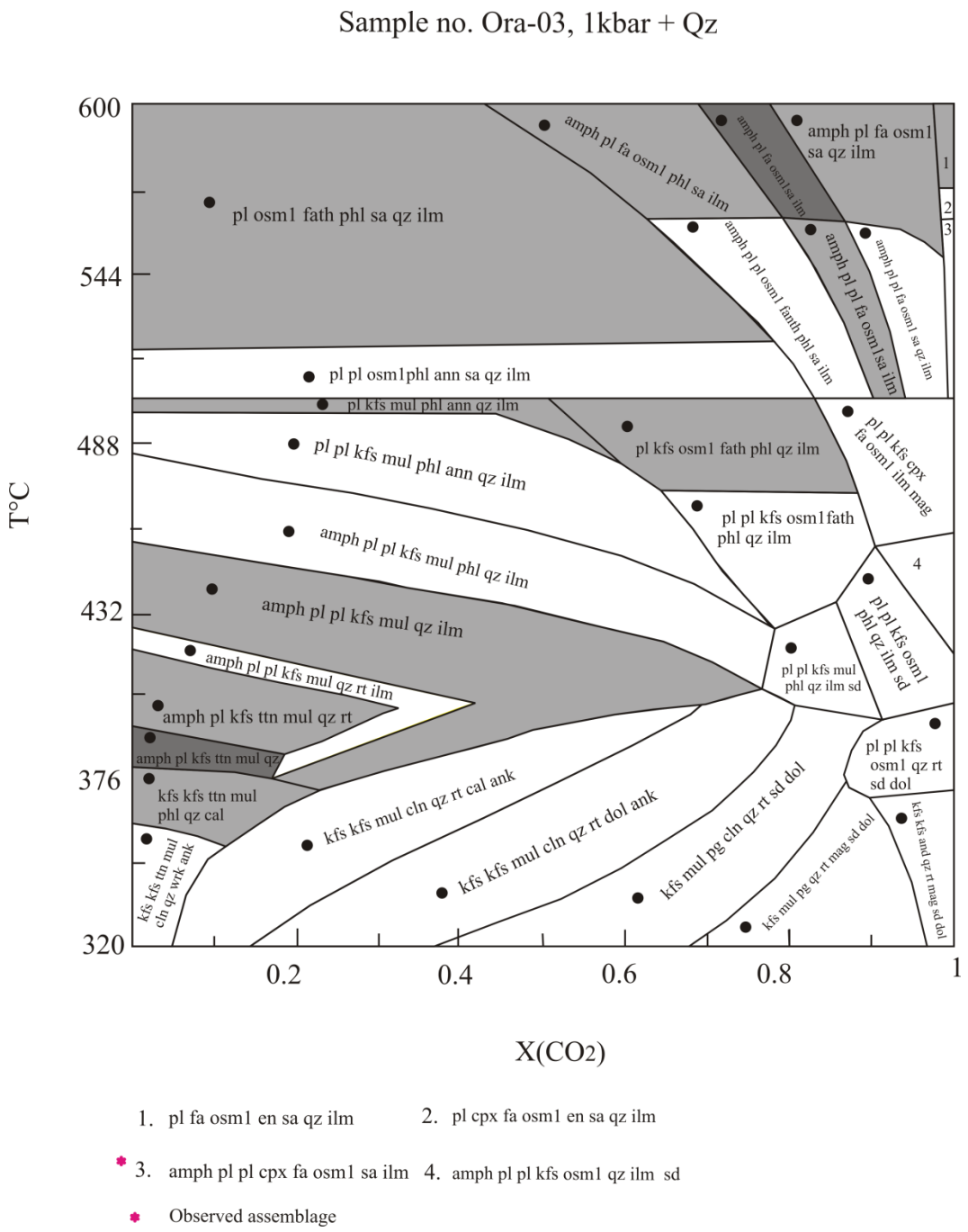

.

Figure 7.1: Isobaric T-$X(CO_2)$ diagram for sample Ora-03 at 1 kbar. Shading represents degrees of variance, such that lighter shades are low variance and darker shades are higher variance.

The equilibrium assemblage amph + cpx + qz + ttn + cal + mc + bt + ep was observed in thin section of Jtng-09 sample and used in pseudosection calculations. In the

pseudosection (Fig.7.2), calcic amphibole, cpx and titanite are in equilibrium within the assemblage observed as 'amph pl cpx ttn sa ilm' which derived the stability field with temperature range of 570°-580°C and fluid compositions of $X(CO_2)$,i.e.0-0.8.Calcic amphibole (actinolite) appears at almost 360°C and destabilizes above 440°C with the appearance of cpx (diopside) which defines the minimum temperature required for its formation and at $X(CO_2)$ range = 0.8 to 1. Calcic amphibole occurs at most of the specified conditions.Quartz is stable in the whole T-$X(CO_2)$ range of interest. Titanite is stable at temperature 320-580°C and at higher $X(CO_2)$ conditions, i.e. > 0.90.

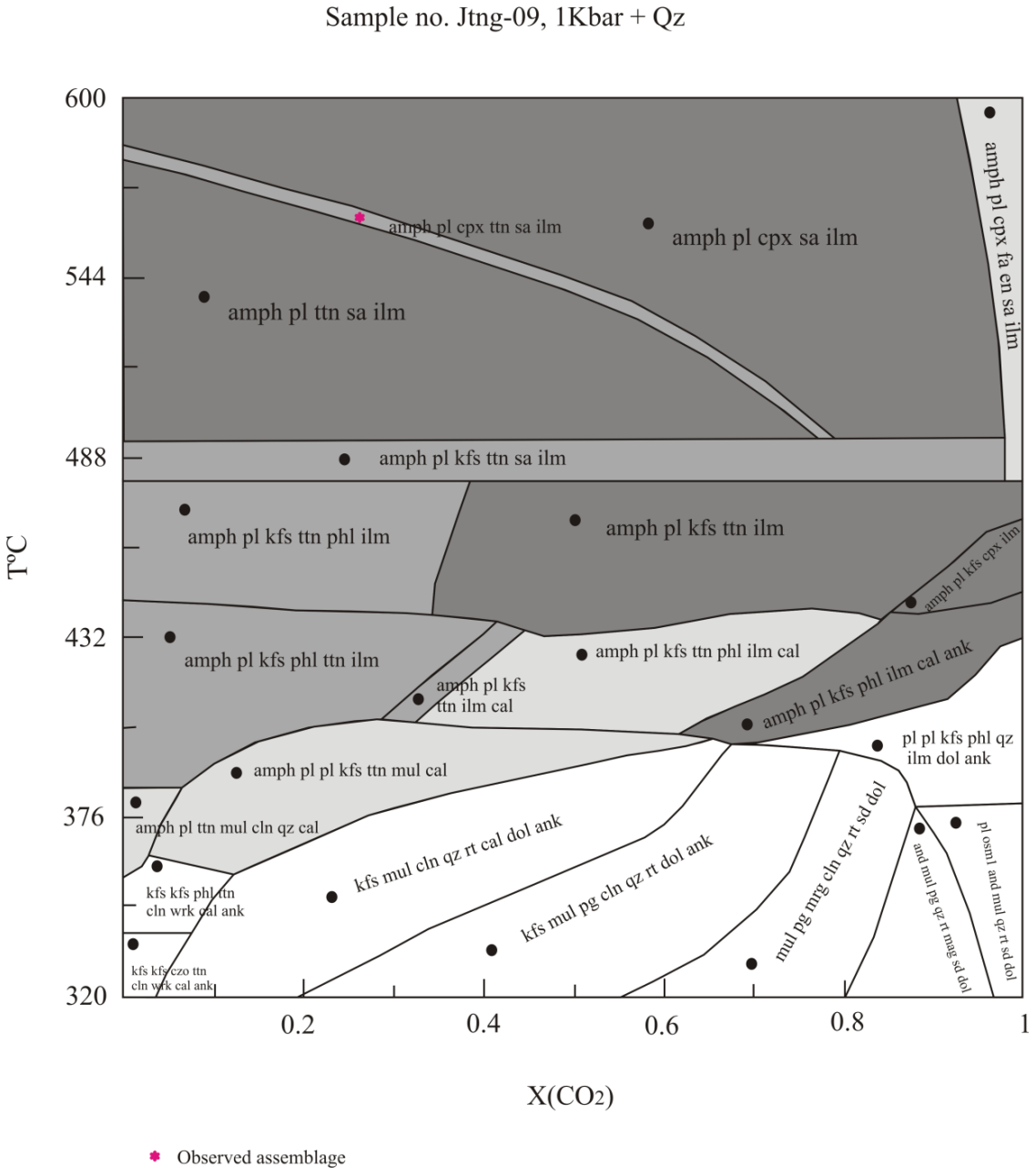

Figure 7.2: Isobaric T-$X(CO_2)$ diagram for sample Jtng-09 at 1 kbar

Carbonate-bearing fields occur over wide range of temperature, i.e. ~320-427° C and almost at all fluid compositions with calcite, ankerite, dolomite and siderite representing a part of protolith composition. K-feldspar (microcline) is predicted in nearly all stability fields, from temperature 320-500°C and almost at all fluid compositions. Phlogopite appears at ~340°C and is stable as part of K-feldspar bearing assemblages upto 480°C and almost at all fluid compositions.Clinozoisite occur at lower and narrow temperature range i.e. at ~ 320-340ºC and H_2O-rich fluid compositions with $X(CO_2) < 0.05$.

The equilibrium assemblage amph + cpx + qz + ttn + cal + mc + bt + ep + pl was observed in thin section of Tlwd-14 sample and used in pseudosection calculations. In the pseudosection (Fig.7.3), calcic amphibole, cpx and plagioclase feldspar are in equilibrium within the assemblage observed as 'amph pl cpx fa en sa ilm' which derived the stability field with temperature range of 500°-620°C and narrow range of fluid compositions i.e. $X(CO_2)$ = 0.8-1.Calcic amphibole (actinolite) appears at almost 370°C and destabilizes above 460°C with the appearance of cpx (diopside) which defines the minimum temperature required for its formation and at $X(CO_2)$ range = 0.8 to 1. Quartz is stable in the whole T-$X(CO_2)$ range of interest. Titanite is stable at narrow temperature range i.e. from 320-430°C and at narrow $X(CO_2)$ conditions i.e < 0.7.

Carbonate-bearing fields occur over wide range of temperature i.e. ~320-470° C and at all fluid compositions with calcite, ankerite, dolomite and siderite representing a part of protolith composition. Potassium-feldspar is predicted in nearly all stability fields, from temperature 320-495°C and at all $X(CO_2)$. Phlogopite appears at ~340°C and is stable as part of various assemblages upto 620°C and almost at all fluid compositions. Clinozoisite occur at lower and narrow temperature range i.e at ~ 320-400ºC and H_2O-rich fluid compositions with $X(CO_2)$ ~0.65. Plagioclase feldspar appears at 370°C and remains stable upto 620°C and at all fluid compositions.

The equilibrium assemblage amph + cpx + cal + qz + ttn + mc + bt + ep + scp was observed in thin section of Bor-P10 sample and used in pseudosection calculations. In the pseudosection (Fig.7.4), calcic amphibole, cpx, plagioclase feldspar and titanite are in equilibrium within the assemblage observed as 'amph pl cpx ttn sa ilm' which derived the stability field with temperature range of 620°-630°C and wide range of fluid compositions i.e. $X(CO_2)$ = 0-0.7.Calcic amphibole occurs at most of the specified conditions excluding low temperatures (below 380°C).

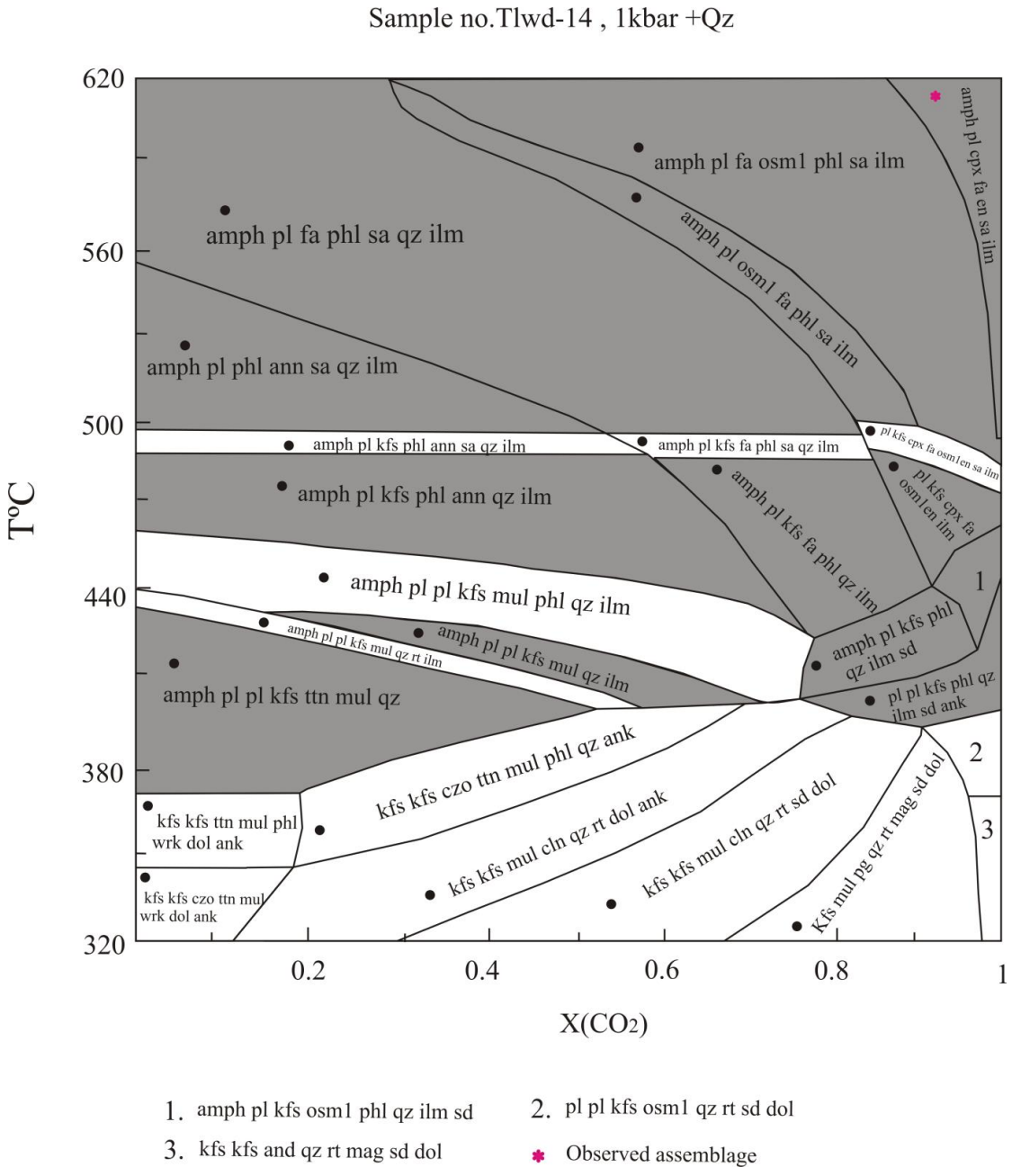

Figure 7.3: Isobaric T-X(CO_2) diagram for sample Tlwd-14 at 1 kbar

The destabilization of calcic amphibole (actinolite) above 450°C and occurrence of Cpx (diopside) defines the minimum temperature of its formation. Cpx is stable at all fluid compositions.

Carbonate-bearing fields occur over wide range of temperature i.e. ~320-430° C and at all fluid compositions with calcite, ankerite, dolomite and siderite representing a part of protolith composition.Quartz is stable in the whole T-X(CO_2) range of interest. Titanite is stable at wide temperature range i.e. from 320-630°C and at wide range of X(CO_2) i.e from 0

-0.95. K-feldspar is predicted in nearly all stability fields, from temperature 320-500°C and at all $X(CO_2)$. Phlogopite appears at ~370°C and is stable upto 430°C and at all fluid composition, $X(CO_2) > 0.7$ Clinozoisite occur at lower and narrow temperature range i.e at ~ 320-375ºC and H_2O-rich fluid compositions of $X(CO_2) < 0.1$.

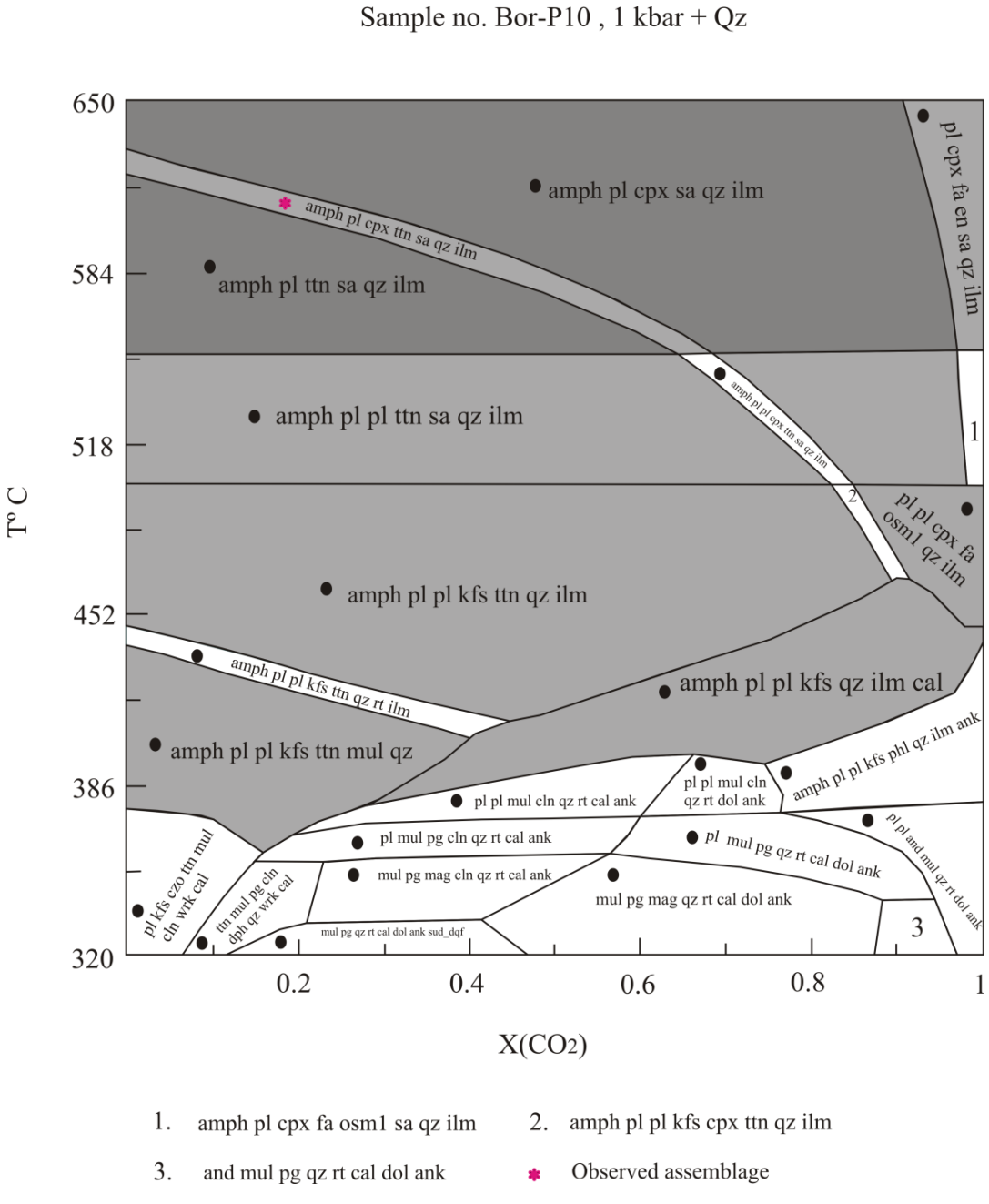

Figure 7.4: Isobaric T-$X(CO_2)$ diagram for sample Bor-P10 at 1 kbar

7.4 Chemographic Projections

The chemographic projections of calc-silicate rocks in the CaO-MgO-SiO_2-H_2O-CO_2 (CMS-HC) system are shown by (Fig.7.5) at 1kbar pressure. These diagrams exhibit the important relationships between rocks and minerals. Chemical compositions of minerals and rocks are portrayed by these diagrams which are useful in phase equlibria studies. In these diagrams, left half represent the carbonate rocks while right half covers the ultramafic rocks (Winter,2010). Progression of metamorphism is presented through the diagrams,i.e. (from Fig. 7.5a to 7.5c). The protolith (calcareous sandstone) with the major assemblage Dol +Cal + Qz might have undergone low grade metamorphism with temperature 350°C, fluid composition, viz. $X(CO_2)$ = 0.3 and at 1kbar on account of which talc mineral appeared (Fig.7.5a). With the further progression of metamorphism with temperature 450°C and $X(CO_2)$ = 0.5, tremolite mineral appeared within Tlc-Qz-Cal sub-triangle (Fig.7.5b) indicating its formation from talc, quartz and calcite. At 550°C and $X(CO_2)$ = 0.7,diopside appeared within Tr-Qz-Cal subtriangle (Fig.7.5c).

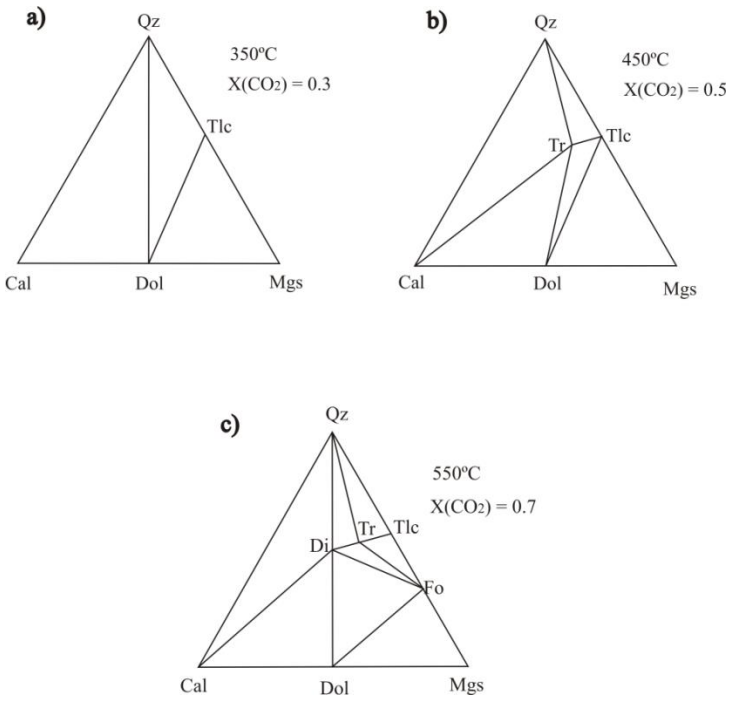

Figure 7.5: The sequence of CMS-HC chemographic diagrams for metamorphosed protolith. a) Appearance of talc mineral by low grade metamorphism of protolith; b) Development of tremolite with progression of metamorphism; c) Appearance of diopside with further progression of metamorphism. All chemographic calculations were conducted in Perple_X v.6.8.1 (Connolly,2005;Connolly,2009) using thermodynamic and end-member compositional data from the Holland and Powell (2003) dataset.

It is clear from previous studies that the Lunavada Group has undergone three phases of deformation, viz. D_1,D_2 and D_3 which led to M_1, M_2 and M_3 metamorphic events. Appearance of chlorite in the northernmost part of the region around Lunavada, biotite in the central part and the garnet in the southernmost part of the region denotes the increase in grade of metamorphism from north to south of the region.

Thus the regional metamorphic facies,i.e. upper greenschist to lower amphibolite facies is indicated for the rocks of this group from north to south (Mamtani,1998). According to him, the thermal event of Godhra Granitic intrusion was experienced by these rocks after regional metamorphism. This event was syn to post D_3. Megascopic and microscopic characteristics of the calc-silicate rocks prove that they have been influenced by later contact metamorphism caused due to this plutonic activity.

The thermobarometry as well as phase equilibria studies revealed the temperature and pressure conditions at peak metamorphism. An average temperature, 634°C and 1.1 kbar of pressure at peak metamorphism points towards the 'Hornblende-hornfels facies' of contact metamorphism for these calc-silicates. This is shown by a symbol '*' in the following temperature-pressure diagram (Fig.7.6).

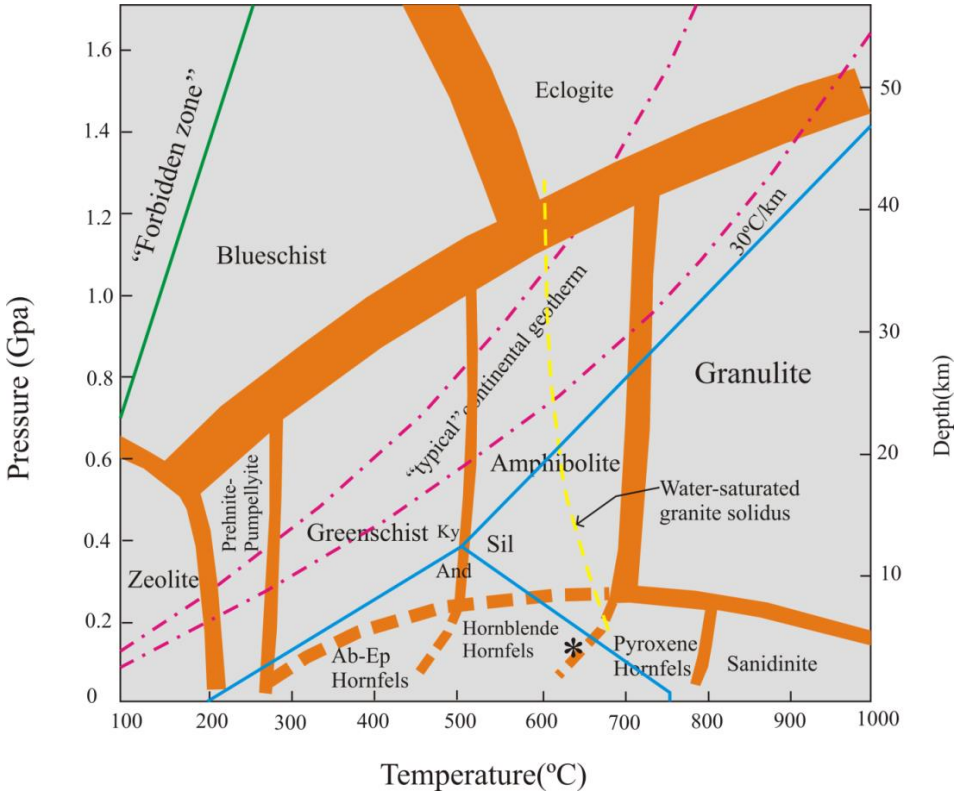

Figure 7.6: The temperature- pressure diagram, (after Winter, 2010).The calc-silicate rocks fall within the 'Hornblende-hornfels facies' of contact metamorphism which is shown by the symbol '*' in the respective field.

7.5 Tectonic implications

The Aravalli Mountain Belt is one of the major Proterozoic accretionary mountain belts of the world. According to (Kaur et al.,2009, 2011, 2013 and Bhowmik et al., 2010), Proterozoic crustal development along with the congregation of the supercontinent Columbia can be better understood with the help of its tectonic evolution.

Using trace element geochemistry and petrofacies analyses, Banerjee and Bhattacharya (1989, 1994) applied the plate tectonic concepts to attribute each of the Aravalli clastic rocks to specific tectonic setting and interpret the evolution of the Aravalli basin in a passive margin setting which later changed to active margin setting. As discussed in preceding sections, the petrological and geochemical characteristics of calc-silicate rocks of the study area around Lunavada region are consistent with their derivation from active continental margin setting which substantiates the depositional history of Aravalli supergroup from passive margin to active margin towards the middle phase of the Aravalli Geological Cycle,i.e. almost at the beginning of Mesoproterozoic age as indicated by the tectonic model of the evolution of the Aravalli basin by (Absar and Sreenivas ,2015).

Generally, it was considered that the Aravalli Supergroup had been deposited during 2.1–1.9 Ga. Similarly, according to (Ahmad and Tarney, 1994; Mallikarjuna Rao et al., 1995; Deb and Thorpe, 2004 and Ahmad et al., 2008), isotopic, geochemical and geochronological studies of the mafic and ultramafic lavas of the Delwara volcanics in the basal Aravalli sequence indicate that the ocean opening of the Aravalli basin was completed by 2.2–2.1 Ga. However, $^{207}Pb/^{206}Pb$ geochronological data of detrital zircons by (McKenzie et al., 2013) firmly rejected an early Palaeoproterzoic age of the Aravalli Supergroup and suggested a late Palaeoproterozoic to Mesoproterozoic age (1.77–1.59 Ga) for these strata, instead.

7.5.1 The tectonic model

In the present study, the evolution of Lunavada basin is proposed through the plate tectonic model of evolution of the Aravalli fold belt that has been portrayed in the following series of cartoons in Fig.7.7. On the basis of geochronological studies of Aravalli Supergroup by (Mckenzie et al.,2013), Absar and Sreenivas (2015) postulated that the formation Aravalli basin was initiated during continental rifting of the BGC protocontinent at 1.83 Ga (Stage 1, Fig.7.7a). The early rift stage is shown by interbedded Delwara mafic volcanics and quartz-arenites. Rifting led to the formation of full-fledged Aravalli oceanic basin with development of oceanic crust. The rift basin gradually evolved into a passive margin during ca. 1.77 Ga

(Stage 2, Fig.7.7b) and deposition of Jhamarkotra carbonates and phosphorites took place in a shallow water carbonate platform along with carbonaceous shales in comparatively deeper water.

a) Stage 1 : Early rift stage leading to the opening of Aravalli basin, (Late Palaeoproterozoic,~1.83 Ga)

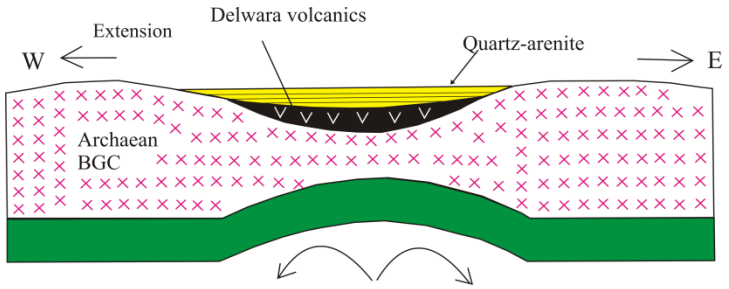

b) Stage 2: Passive margin stage,(1.77 Ga)

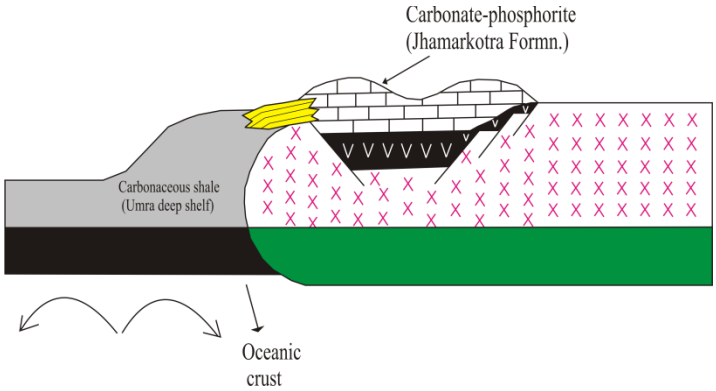

(c) Stage 3: Formation of accretionary prism due to subducting oceanic crust towards east,(1.64-1.59 Ga)

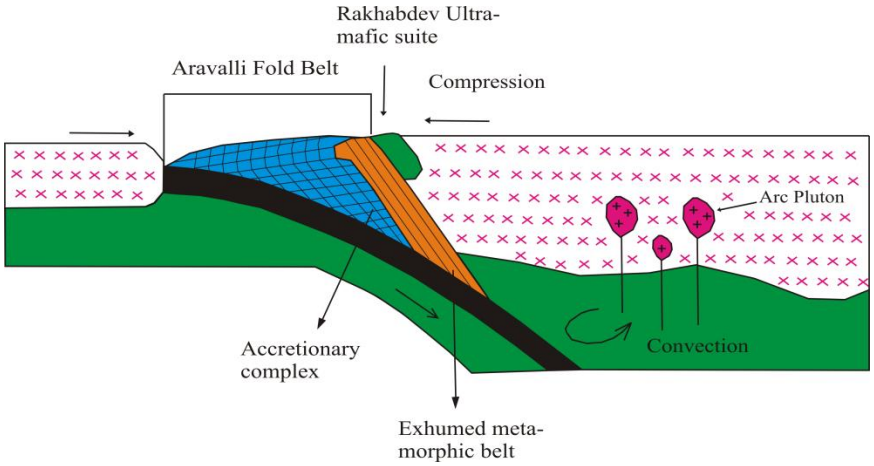

d) Stage 4: Crustal extension due to slab roll back giving rise to back arc basin, (~1.59 Ga)

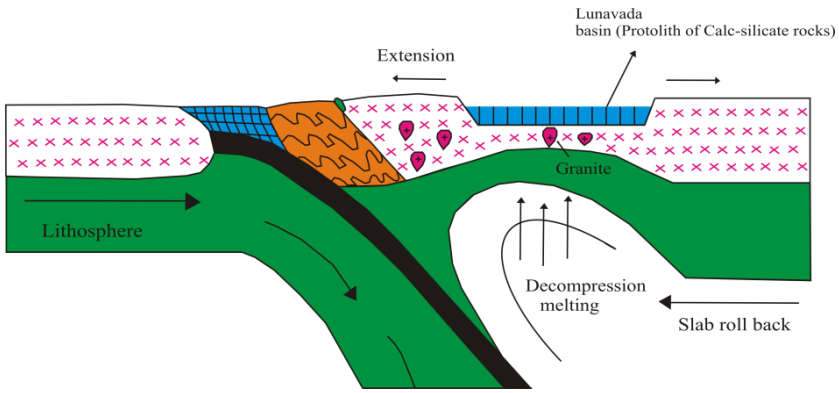

Figure 7.7: Cartoon diagrams showing the different stages of evolution of the Lunavada basin, NW India. a) Stage 1, (~1.83 Ga) : Rifting led to the opening of Aravalli basin, b) Stage 2, (1.77 Ga) : Passive margin stage with deposition of Jhamarkotra carbonates and phosphorites in a shallow water along with deposition of carbonaceous shales in comparatively deeper water, c) Stage 3, (1.64-1.59 Ga) : Eastward subduction of oceanic crust leading to the development of accretionary prism, d) Stage 4, (~1.59 Ga): Crustal extension giving rise to back arc basin (Lunavada basin), (modified after Bhowmik and Dasgupta, 2012 ; Absar and Sreenivas,2015).

Banerjee and Bhattacharya (1994) contemplated the closure of the Aravalli ocean due to westward subduction of Aravalli oceanic crust and collision of the Aravalli continental margin with the arc-microcontinent along the Rakhabdev lineament. However, According to (Absar and Sreenivas,2015), these models suffer from certain drawbacks such as (1) these do not explain the formation of linear Aravalli sub-basins at the Bhilwara terrain during the tectonic cycle, (2) tectonic episodes are wrongly interpreted because of inappropriate stratigraphic correlation of various litho-units of the Aravalli Supergroup, wherein the Upper Aravalli Debari Formation is being considered as the basal horizon (e.g. Roy et al., 1993; Roy and Jakhar 2002), and (3) these do not provide a unified tectonic model for basin evolution and formation of mineral deposits. Hence they supported a concept of eastward subduction of Delwara oceanic crust beneath the BGC continent in an Andean-type plate margin on the basis of recent geochemical dataset, more refined stratigraphic record of the Aravalli Supergroup (Roy and Jakhar 2002), and recent detrital zircon U-Pb ages (McKenzie

et al., 2013) of Aravalli clastic rocks and reconstructed the tectonic model of Aravalli basin accordingly.

Accretionary orogenesis caused an eastward subduction of Aravalli oceanic crust with the development of 'Aravalli fold belt' during ca.1.64 -1.59 Ga. It covers the exhumed metamorphic belt along with Rakhabhdev Ultramafics on its east (Stage 3, Fig.7.7c). Palaeoproterozoic accretionary orogenesis continued (Stage 4, Fig.7.7d) and here, it is postulated that at almost towards the end of the above time frame or at the end of active stage i.e. at ca 1.59 Ga a new cycle of crustal extension started with the formation of Lunavada sub-basin. This process led to the simultaneous compression in response to sequential slab roll-back and slab advancement movements. A statement by (Gupta et al., 1997) that the formation of Lunavada basin was late to post orogenic phase of the Aravalli Supergroup is also in agreement with this model. The cycle led to the formation of the protoliths of the calc-silicate rocks of Lunavada in possible back-arc enviroment. Intrusion of continental arc plutonic activity (Granite) caused the thermal metamorphism of the protolith of present day calc-silicate rocks.

---------- *END* ----------